Brain Research Bulletin 116 (2015) 57–66

Contents lists available at ScienceDirect

Brain Research Bulletin

journal homepage: www.elsevier.com/locate/brainresbull

Long lasting cerebellar alterations after perinatal asphyxia in rats

Verónica Campanille, G. Ezequiel Saraceno[1], Stéphanie Rivière, Tamara Logica, Rodolfo Kölliker, Francisco Capani, Rocío Castilla*

Instituto de Investigaciones Cardiológicas "Prof. Dr. Alberto C. Taquini" (ININCA), UBA-CONICET, Marcelo T. de Alvear 2270, C1122AAJ Buenos Aires, Argentina

ARTICLE INFO

Article history:
Received 18 February 2015
Received in revised form 27 May 2015
Accepted 20 June 2015
Available online 24 June 2015

Keywords:
Cerebellum
Perinatal asphyxia
Cerebellar cortex
Hypoxia

ABSTRACT

The developing brain may be particularly vulnerable to injury before, at and after birth. Among possible insults, hypoxia suffered as a consequence of perinatal asphyxia (PA) exhibits the highest incidence levels and the cerebellar circuitry appears to be particularly susceptible, as the cellular makeup and the quantity of inputs change quickly during days and weeks following birth.

In this work, we have used a murine model to induce severe global PA in rats at the time of birth. Short-term cerebellar alterations within this PA model have been previously reported but whether such alterations remain in adulthood has not been conclusively determined yet. For this reason, and given the crucial cerebellar role in determining connectivity patterns in the brain, the aim of our work is to unveil long-term cerebellum histomorphology following a PA insult.

Morphological and cytological neuronal changes and glial reaction in the cerebellar cortex were analyzed at postnatal 120 (P120) following injury performed at birth. As compared to control, PA animals exhibited: (1) an increase in molecular and granular thickness, both presenting lower cellular density; (2) a disarrayed Purkinje cell layer presenting a higher number of anomalous calbindin-stained cells. (3) focal swelling and marked fragmentation of microtubule—associated protein 2 (MAP-2) in Purkinje cell dendrites and, (4) an increase in glial fibrillary acidic protein (GFAP) expression in Bergmann cells and the granular layer.

In conclusion, we demonstrate that PA produces long-term damage in cellular histomorphology in rat cerebellar cortex which could be involved in the pathogenesis of cognitive deficits observed in both animals and humans.

1. Introduction

The developing brain may be particularly vulnerable to maternal stress and to other environmental insults before, at and after birth (Kinney et al., 2008; McEwen, 2007). Among these insults, hypoxia suffered as a consequence of perinatal asphyxia (PA) appears to be one of the most important stressful factors.

Brain injury induced by PA is one of the most frequent causes of morbidity and mortality in term and preterm neonates, accounting for 23% of neonatal deaths globally (Lawn et al., 2005). Following PA, approximately 45% of newborns die and 25% have permanent neurological deficits including motor and cognitive alterations of variable severity, such as seizures, spasticity, eyesight and hearing impairment, attention deficit, hyperactivity, mental retardation and other neuropsychiatric syndromes with delayed clinical onset (de Haan et al., 2006; du Plessis and Volpe, 2002; Kaufman et al., 2003; Odd et al., 2009; Titomanlio et al., 2011; Van Erp et al., 2002; Vannucci and Hagberg, 2004). PA thus interferes with neonatal development, generating long-term mental and neurological deficits whose underlying mechanisms have not been fully elucidated yet.

Histologically, brain injury occurring early during development results in significant damage in different areas of the central nervous systems (CNS). In particular, hypoxia/ischemia as consequence of PA causes damage in cerebellum, hippocampus, neostriatum and substantia nigra (Capani et al., 2009). The

Abbreviations: PA, perinatal asphyxia; PCs, Purkinje cells.

* Corresponding author.
E-mail addresses: vcamp@fibertel.com.ar (V. Campanille), ezequiel.saraceno@u-bordeaux.fr (G.E. Saraceno), s.riviere86@gmail.com (S. Rivière), logicamente.tam@gmail.com (T. Logica), rodolfo@kollikerfrers.com.ar (R. Kölliker), fcapani@fmed.uba.ar (F. Capani), rcastillalozano@fmed.uba.ar (R. Castilla).
[1] Present address: Interdisciplinary Institute for Neuroscience (IINS), University of Bordeaux, Bordeaux, France. UMR 5297, Centre National de la Recherche Scientifique (CNRS), Bordeaux, France.

http://dx.doi.org/10.1016/j.brainresbull.2015.06.003
0361-9230/

mechanisms for brain injury after hypoxia/ischemia care thought to include energy failure, free radical damage, cytokine release and excitotoxicity, and caspase-dependant cell death (Barks and Silverstein, 1992; Cheng et al., 1998; Hagan et al., 1996; Liu et al., 1996; O'Lone et al., 2007).

The type and distribution of human brain lesions differ markedly between premature and term babies, likely as a consequence of differences in brain maturation and regional vulnerability, as described in different previous studies (Miller and Ferriero, 2009; Verger et al., 2001a,b; Yager and Thornhill, 1997). The immaturity of a particular brain region is highly relevant, as the insult affects the initial plastic changes required for establishing neurocircuitries and synaptogenesis (Anderson et al., 2011). In this sense, the cerebellum is particularly vulnerable because, in humans, it reaches its mature volume within months of birth (Rice and Barone, 2000) and develops throughout pregnancy with rapid growth in the third trimester and in the first postnatal year (Limperopoulos et al., 2007; ten Donkelaar et al., 2003; Zervas et al., 2005). During days and weeks following birth, the cerebellar circuitry is susceptible to injury (ten Donkelaar et al., 2003), as the cellular makeup and the quantity of inputs change quickly (Wang and Zoghbi, 2001). Moreover, it has been demonstrated that brain injury derived from premature birth is associated with cerebellar growth impairment (Limperopoulos et al., 2005).

Traditionally, the role of the cerebellum has been associated to the coordination of voluntary movement, gait, posture, speech and motor functions (Ghez and Fahn, 1985) and has not been considered relevant to the field of psychiatry or the study of brain–behavior relationships. However, growing evidence shows that the cerebellum may play a role in cognition, behavior and psychiatric illness (Glickstein, 2006).

In recent years, we have used a murine model to induce severe global PA in rats at the time of birth, as this model offers three key advantages: first, it mimics relevant aspects of human delivery in an adequate way; second, as it is a non-invasive procedure, it allows for the study of both short and long-term effects; third, it is easily reproducible across laboratories (Capani et al., 2001). Short-term cerebellar alterations within this model of PA have been previously reported (Biran et al., 2011, 2012) but whether such alterations remain in adulthood has not been conclusively determined yet. For this reason, and given the crucial cerebellar role in determining connectivity patterns in the brain, the aim of this paper is to unveil long-term cerebellum morphologycal alterations following a perinatal asphyctic–ischemic insult. To this end, modificacions in the structural organization of the cerebellar cortex were analyzed in young adulthood rats (P120) following injury performed at birth (P0).

2. Material and methods

2.1. Animals

All procedures involving animals were approved by the Institutional Committee of Animal Care and Use at the University of Buenos Aires (CICUAL, School of Medicine) and conducted according to the principles of the Guide for the Care and Use of Laboratory Animals (NIH Publications No. 80-23, revised 1996).

Female Sprague-Dawley rats in the fifteenth day of pregnancy were placed in individual cages and maintained on a 12:12 h light/dark cycle in a temperature- ($21 \pm 2\,^{\circ}C$) and humidity-controlled ($65 \pm 5\%$) environment. Animals had access to food (Purina chow) and tap water ad libitum and were divided in 3 groups: (1) surrogate mothers ($n = 3$), (2) mothers of control pups ($n = 3$) and (3) mothers assigned to PA ($n = 4$).

2.2. Induction of asphyxia

The induction of asphyxia was carried out as previously described (Saraceno et al., 2010). At the time of delivery, a first spontaneous birth was allowed, dams were rendered unconscious by CO_2 inhalation and rapidly killed by decapitation and subjected to a caesarean section and hysterectomy (Dorfman et al., 2006). The uterus horns containing the fetuses were immediately immersed in a water bath at 37 °C for 19 min (sub-severe PA) (Bjelke et al., 1991; Capani et al., 2009; Van de Berg et al., 2003). Following asphyxia, the uterus horns were rapidly opened and the male pups removed, cleaned and then resuscitated by intermittent tactile breathing stimulation for a few minutes until regular pulmonary breathing was established. The umbilical cord was then ligated and animals were left to recover for 1 h under a heating lamp. They were then given to surrogate mothers and mixed in with male control pups (10 pups total per surrogate mother) until the end of the study.

Asphyxia was administered for 19 min, as 21 or more minutes in this condition results in survival rates under 3% (Capani et al., 2009).

Animals born by natural delivery were used as controls to avoid alterations produced by the short time of exposure to CO_2, which may be similar to the injury produced by asphyxia.

2.3. Histological examinations

Four-month-old rats were anaesthetized (Nembutal 50 mg/kg body weight, i.p.) and perfused transcardially with 30–50 ml of 0.1 M phosphate buffered saline (pH 7.4) (PBS) containing 4% paraformaldehyde. Cerebella were removed and post-fixed in the same fixative solution for 2 h at room temperature, and then immersed in 0.1 M phosphate buffer (pH 7.4) containing 20% sucrose at 4 °C overnight. Cerebella were then paraffin-embedded, cut in 4-μm-thick sagittal sections, dewaxed by xylene and hydrated by successive immersion in ethanol 100%, 96%, 70% and water.

2.4. Immunohistochemistry

After antigen retrieval with 0.01 M citrate buffer pH 6, endogenous peroxidase activity was blocked by incubation in 3% hydrogen peroxide in 60% methanol. Non-specific binding sites were blocked with 5% bovine serum albumin. Sections were incubated overnight at 4 °C with a rabbit polyclonal anti-Glial fibrillary acidic protein antibody (anti-GFAP, 1:500; Sigma Louis, MO, USA), anti-microtubule-associated protein 2 (MAP-2 1:250; Sigma St. Louis, MO, USA), anti-neuron-specific nuclear protein (anti-NeuN, 1:100; Millipore, Chemicon, CA, USA) or anti- calcium-binding protein calbindin-D28k (anti-calbindin D28K, 1: 250; Santa Cruz Biotechnology, Inc.). After several washes, sections were incubated with secondary antibodies (biotinylated anti-rabbit IgG or biotinylated anti-mouse IgG, Vector Laboratories Inc., Burlingame, CA, USA) for 2 h at room temperature.

To reveal the sites of antigen/antibody binding, an avidin-horseradish peroxidase complex (Vector Laboratories, Burlingame, CA, USA) and the chromogen 3,3′-diaminobenzidine tetrahydrochloride (DAB; Sigma, St. Louis, MO, USA) were used.

For control staining, some sections were incubated with PBS instead of the primary antibody and no immunoreactivity was detected. Sections were dehydrated in ethanol, cleared in xylene and mounted in Canada balsam, and then photographed using Nikon Eclipse 80i microscope and Visiopharm Integrator System software.

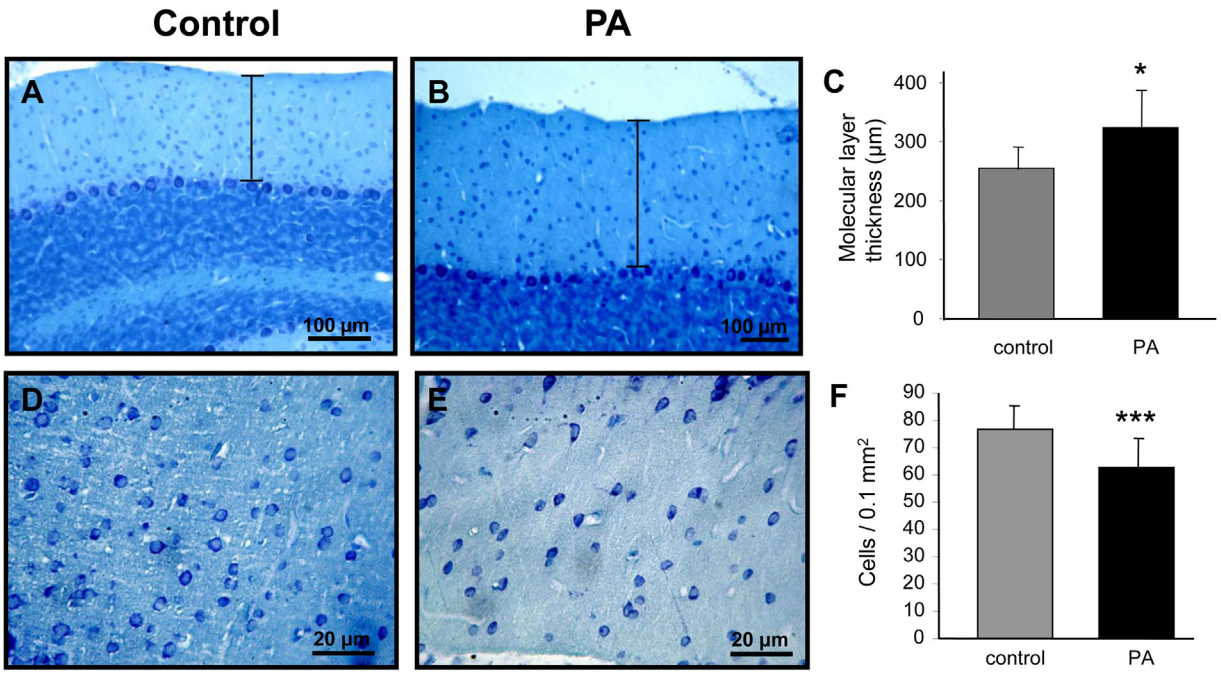

Fig. 1. Molecular layer. Panels A, B, D and E show representative microphotographs of toluidine blue-stained molecular layer from control and PA animals. Panels A and B show differences in molecular thickness (bars indicate how measurements were done) and quantification is shown in panel C. Panels D and E show differences in cell number (quantification per area shown in panel F). Data are expressed as the mean ± SD of a single experiment (Control: $n = 12$, PA: $n = 12$). $^{*}p < 0.05$, $^{***}p < 0.001$, compared to control.

2.5. Planimetric studies

In all cases, the material examined was processed at the same time with same solutions, to avoid differences by deformation of biological tissues.

The sagittal sections analyzed were between 1.13 and 1.40 mm of distance from the midline according to the Atlas by Paxinos and Watson.

We determined cell number per area using the "Cell Counter" Image J plug-in tool. Molecular layer cells were quantified from 25× magnification micrographs in a grid considering 4 squares of 10,000 μm^2 each (total surface 40,000 μm^2 = 0.04 mm) in each picture in such a manner that the whole area was represented.

Granular layer cells were quantified from 100× magnification photographs in a grid considering 4 squares of 250 μm2 (total surface of 2000 μm2 = 0.002 mm) in each picture.

In all cases the relative position of the counting grid was randomized to provide an unbiased sample. Subsequently, we calculated the number of cells per mm^2.

To assess the linear density of Purkinje cells, we quantified cells in a length determined by means of the "Straight" tool in Image J software.

All material was examined by a team member who was blind to clinical and pathological data.

2.6. Preparation of tissue extracts for western blot

Frozen cerebella were homogenized (200 mg/ml) in an RIPA buffer (50 mM Tris–HCl (pH 7.4), 1 mM EDTA, 1% Triton ×-100, 1% sodium deoxycholate, 0.1% SDS) containing protease inhibitors (1 mM PMSF, 5 μg/ml aprotinin, 5 μg/ml leupeptin). Cerebella were then sonicated at 4 °C, three times for 15 s. each in RIPA buffer in the absence of detergents. Detergents were later added and cerebella were incubated for 2 min at 4 °C and then centrifuged at 12,000 rpm at 4 °C for 15 min. (Sorvall RMC14 centrifuge). Supernatants were collected and the protein content of each sample was determined by the Bradford micro-method using bovine serum albumin as standard (Bio-Rad, Hercules, CA, USA).

2.7. Western blot analysis

Proteins were separated by SDS-PAGE and transferred to poly(vinylidene difluoride) (PVDF) membranes (Bio-Rad Laboratories Inc., Hercules, CA, USA).

GFAP protein, calbindin-D28k and actin were detected using anti-GFAP antibodies (Sigma St. Louis, MO, USA), anti-calbindin D28k (Santa Cruz Biotechnology, Inc.) and anti-β-actin (clone AC-15 from Sigma St. Louis, MO, USA), respectively, and enhanced chemiluminescence reagents (GE Healthcare, Chalfont St Giles, UK). For quantitative analysis, band intensities were analyzed using ImageQuant 5.2 software.

2.8. Statistical analysis

Material from 12 rats for each experimental group was analyzed. All statistical analyses were performed by two-way analysis of variance (ANOVA). When interaction effects were significant, analyses of the simple effects were carried out by post hoc comparisons using *t*-test. Results were expressed as the mean ± SD. Differences with a probability of 5% or less were considered to be significant ($p < 0.05$). All statistical analyses were done using the PASW Statistics 18 software (SPSS Inc., Chicago, IL, USA).

3. Results

With the aim of evaluating neuronal histological and cytological changes and glial reaction in the cerebellar cortex, we analyzed cerebella from four-month-old rats submitted to PA. We evaluated the different structures of the cerebellar cortex of 12 animals of each group, control and PA.

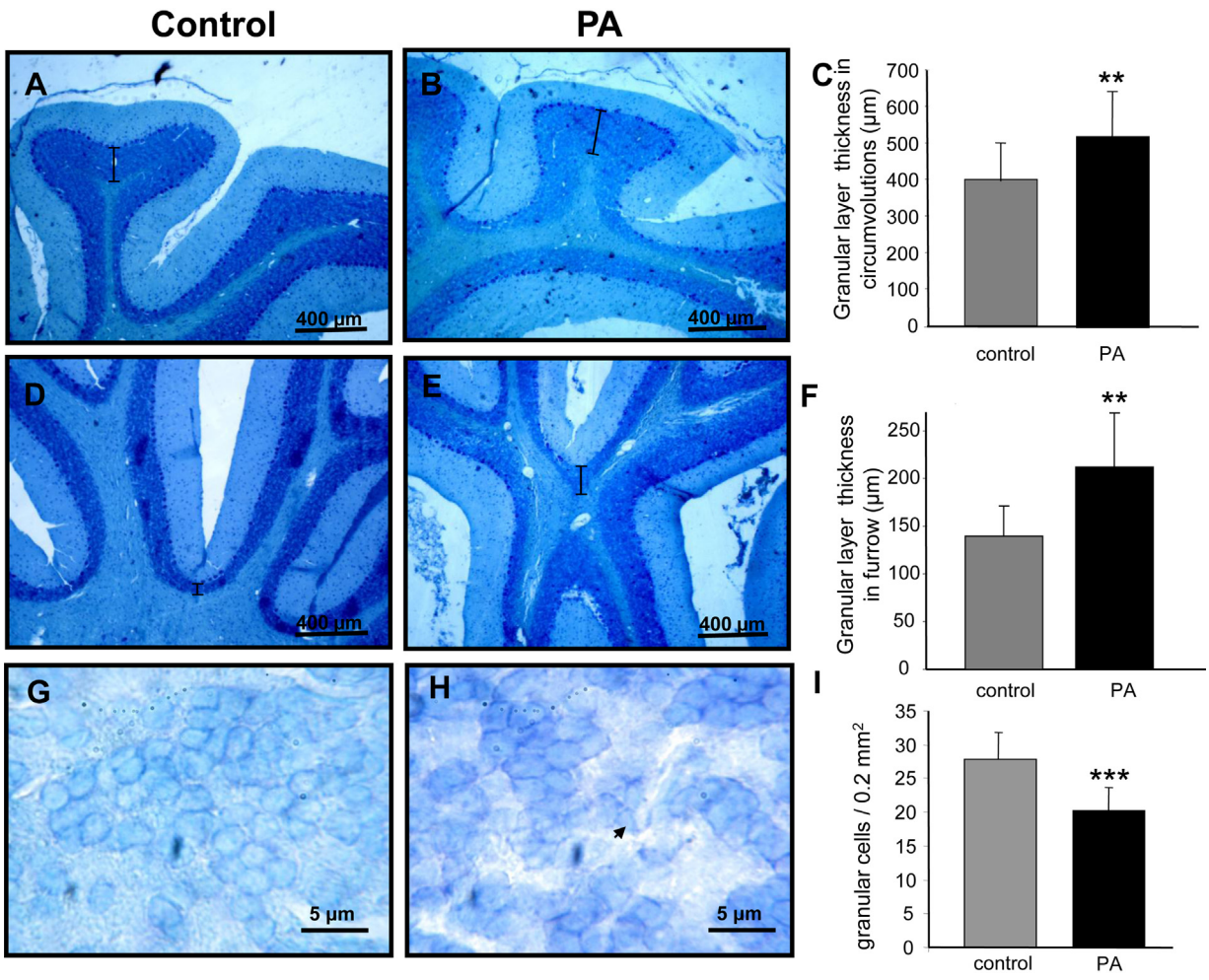

Fig. 2. Granular layer. Panels A, B, D, E, G and H show representative microphotographs of toluidine blue-stained granular layer from control and PA animals. Panels A and B, show differences in granular layer thickness in circumvolutions (quantification shown in panel C). Panels D and E show differences in granular layer thickness in furrows (quantification shown in panel F). In all cases bars indicate how measurements were done. Panels G and H show differences in cell number (quantification per area shown in panel I). Arrow indicates a cell with a smaller nucleus. Data are expressed as the mean ± SD of a single experiment (Control: $n = 12$, PA: $n = 12$). $^{**}p < 0.01$, $^{***}p < 0.001$, compared to control.

3.1. Molecular layer thickness

Molecular layer thickness was measured in photographs of toluidine blue-stained slices. To this end, at least 5 measurements were done in each photograph (10 photographs per cerebellum), see representative images in Fig. 1A and B. As shown in Fig. 1C, a significant increase in layer thickness was determined in PA animals as compared to controls ($p < 0.05$).

Interneurons (basket and stellate cells) and glia in the molecular layer (see representative images in Fig. 1D and E) were then quantified as toluidine blue-positive nuclei present in an area of 0.1 mm^2 (Fig. 1F). Results revealed an 18.7% reduction in cell density in PA animals as compared to controls ($p < 0.001$). However, no significant differences were obtained between controls and PA animals when the number of cells in each group was multiplied by the corresponding molecular layer thickness, indicating no reduction in the total number of cells in the cerebellar molecular layer from PA rats (data not shown).

3.2. Internal granular layer

Internal granular layer thickness was also measured in photographs of toluidine blue-stained slices. In this case, and considering the heterogeneity observed in this layer, we discriminated between measurements registered in cerebellar circumvolutions and those registered in furrows (see representative microphotographs of circumvolutions in Fig. 2A and B, and of furrows in Fig. 2D and E). In both, circumvolutions, the granular layer (Fig. 2C) was significantly thicker ($p < 0.05$) in the PA group as compared to controls. A similar result ($p < 0.01$) was obtained when measurements were done in furrows (Fig. 2F).

The number of toluidine blue-stained cells, i.e. granular, Golgi and glia cells, were also evaluated in the granular layer (Fig. 2G and H) in an area of 0.2 mm^2. PA animals showed a 27.5% reduction in cell density as compared to controls ($p < 0.001$) (Fig. 2I). Nevertheless, when the number of cells in each group was multiplied by the mean granular layer thickness, no significant differences were obtained between control and PA animals, which suggest no reduction in the total number of granular layer cells in PA rats (data not shown).

From the morphological point of view, neurons in the granular layer of control cerebella showed round, dark, homogenously stained nuclei which appeared to be tightly packed, whereas cerebella from rats which had suffered a 19-min asphyctic insult revealed a significant ($p < 0.001$) increase in percentage of cells presenting dysmorphically shaped nuclei (oval, polygonal) (control: 3.09 ± 1.12 vs PA: 8.6 ± 2.34).

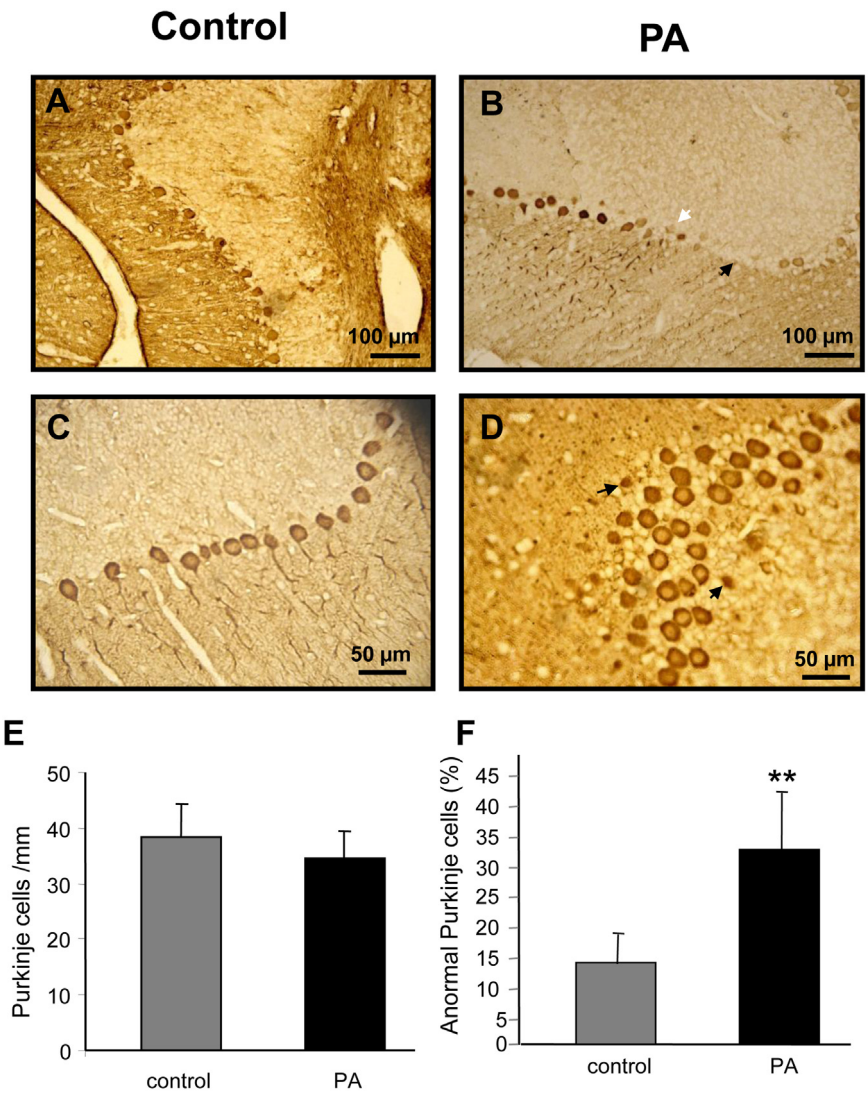

Fig. 3. Purkinje cells. Panels A–D show representative microphotographs of Calbindin-stained PCs from control (panels A and C) and PA (panels B and D) animals. Black arrows indicate morphologically altered cells and white arrow indicates a cell with negative calbindin staining. The quantification of PCs is shown in panel E. The proportion of abnormal PCs in each group is shown in panel F. Data are expressed as the mean ± SD of a single experiment (Control: $n = 12$, PA: $n = 12$) $^{**}p < 0.01$, compared to control.

3.3. *Purkinje cells*

Purkinje cells (PCs) constitute the sole output neurons in the cerebellar cortex and thus have a central functional role in integration. For this reason, we analyzed PC number, distribution and morphology by means of immunostaining of calcium-binding protein calbindin (using anti-calbindin-D28k), which is expressed abundantly in Purkinje cells (Celio, 1990).

In terms of PC layer morphology, PA animals showed a disarrayed distribution, in which some areas appeared as a double layer and others presented PC gaps or clusters (Fig. 3A–D). PCs were quantified in cerebella from control and PA animals by counting calbindin-positive cells present in 1 mm of cell layer (linear density). Also, we discriminated between cells exhibiting regular somatic calbindin staining and those showing irregular calbindin staining, such as weak or punctuate somatic localization, or even lack of staining in the cell soma. No significant alterations in the number of PCs were detected in cerebella from PA animals compared to controls (Fig. 3E). However, a higher number of PCs with alterations in calbindin distribution was detected in PA rats ($p < 0.01$, Fig. 3F). Of note, a higher number of cells with altered morphology were obtained when slices were stained with toluidine blue (data not shown).

We also analyzed calbindin-D28k expression by Western blot, which revealed a significant decrease ($p < 0.05$) in cerebella from PA rats as compared to controls (Fig. 4A and B).

In order to study PC dendritic morpholology, immunodetection of MAP-2 was conducted and the molecular layer was analyzed. Animals subjected to PA showed focal swelling and marked fragmentation of MAP-2 as compared to control animals (Fig. 5A and B). In addition, and in order to analyze dendritic ramification, the MAP-2 reactive area was determined in each of the following equal-size molecular layer sections: (1) external, closer to PC soma (Fig. 5C), (2) middle (Fig. 5D), and (3) external (Fig. 5E). Statistical analyses revealed a significant increase in the reactive area in all subdivisions of the molecular layer studied in PA animals. Moreover, the ratio between the internal and external areas indicated no significant differences regarding control group (Fig. 5F).

3.4. *Astrocytes*

It is well established that astrocytes proliferate and the expression of GFAP increases under neurodegenerative conditions.

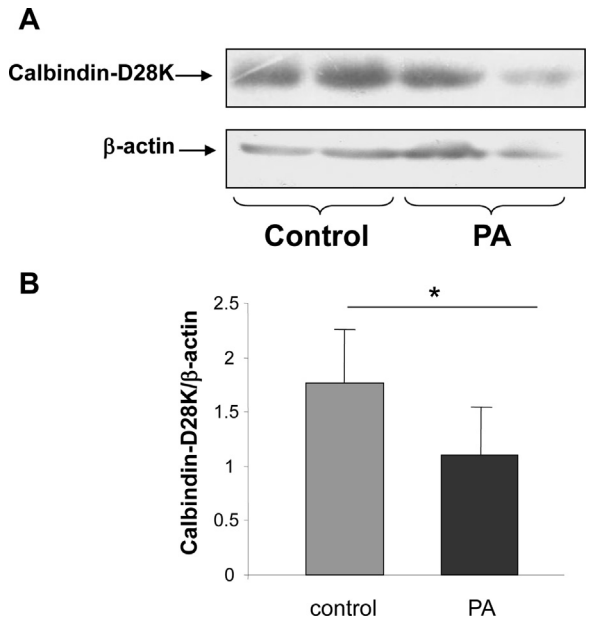

Fig. 4. Cerebellar calbindin expression. Panel A shows representative Western blot for cerebellar calbindin. Panel B shows the quantification of band intensity of three independent experiments. Data are expressed as the mean ± SD. $^*p < 0.05$, compared to control. (Control: $n = 6$, PA: $n = 6$).

Thereby, cerebellar GFAP expression was analyzed by Western blot and revealed a significant increment ($p < 0.001$) in cerebella from PA rats as compared to controls (Fig. 6A and B).

Furthermore, the study of astrocyte morphology by GFAP immunostaining (Fig. 6C and D) showed an increase in the GFAP-positive area in Bergmann cells ($p < 0.001$, Fig. 6E). Finally, the evaluation of GFAP-positive astrocytes in the granular layer (Fig. 6F and G) rendered an increase in the GFAP-positive area ($p < 0.001$) in PA animals as compared to controls (Fig. 6H).

4. Discussion

The present study demonstrates that a hypoxia/ischemia injury shortly after birth produces long-term damage in the histomorphology of rat cerebellum.

To analyze these chronic cerebellar alterations, we used a birth-time hypoxia model in rats, which is suitable for studying the early and late phases of PA. This model mimics relevant aspects of human delivery, as it implies a hypoxic/ischemic insult but no additional lesions such as vessel occlusion (Seidl et al., 2000). This oxygen supply interruption causes brain injury by producing energy failure, free radical damage, cytokines, excitotoxicity and caspase-dependent cell death, among others (Barks and Silverstein, 1992; Cheng et al., 1998; Hagan et al., 1996; Liu et al., 1996; O'Lone et al., 2007).

At birth, the second wave of neuronal cerebellar proliferation plays a key role in the organization of the cerebellar cortex, which makes this brain region particularly vulnerable to insult (Volpe, 2009). Although adaptative mechanisms protect the immature brain from hypoxic damage, severe insults can trigger self-sustaining damaging cascades lasting for days or weeks and resulting in prominent injury (Gonzalez and Ferriero, 2008). In particular, a large body of evidence indicates that PCs are significantly vulnerable to ischemia (Cervos-Navarro et al., 1991; Welsh et al., 2002), as the excessive activation of the *N*-methyl-D-aspartate (NMDA) receptor leads to an increase in intracellular calcium and free radicals, thus triggering hypoxia-induced neuronal damage.

Of note, our findings revealed chronic histological alterations in neurons and glia in the cerebellar cortex of rats suffering PA. These rats also exhibited a disorganized PC layer, alterations in the cellular localization pattern of calbindin and anomalous toluidine blue staining.

Defining PA-affected developmental pathways and establishing molecular targets involved in the disorganization of the PC layer cytoarchitecture have proven to be elusive goals. The formation of the PC layer is a complex process requiring the interaction of various neuronal populations and precise migratory patterns established under glial guidance. PCs are generated during the early embryonic period from the ventricular zone facing the fourth ventricle (Miale and Sidman, 1961) and migrate toward the pial side to subsequently form the PC monolayer during the early postnatal days (Rakic and Sidman, 1970). Therefore, the presence of PCs in heterotopic sites can be a consequence of defective neuronal migration in the developing cerebellum.

A similar interpretation was proposed by Laure-Kamionowska and Maślińska in a large study on cerebellar morphological features in perinatal life. In fact, these authors regarded the frequent finding of irregularly dispersed PCs in the molecular and granular layers as a loss in proper migration (Laure-Kamionowska and Maslinska, 2011).

Calbindin is one of the major calcium-binding and buffering proteins and has a critical role in preventing neuronal death as well as maintaining calcium homeostasis. In our work, PA rats showed a higher number of PCs with irregular calbindin distribution. This irregularity could be the consequence of an alteration in PC morphology as a result of the perinatal insult, as indicated by changes observed in toluidine blue staining experiments. However, some PCs did show a reduction in calbindin expression. The reduction in calbindin expression in animals suffering PA was also confirmed by means of Western blot analysis. A similar result was obtained by Katsetos et al. (2001) who studied this protein expression in hypoxic guinea pig fetus at term. The hypoxia-induced reduction in calbindin-D28k expression could limit neuronal Ca^{2+} buffering capacity, resulting in activation of Ca^{2+} -mediated pathways.

Alterations in dendrites are also a common finding under neurodegenerative conditions (Hori and Carpenter, 1994; Hsu and Buzsaki, 1993; Ikonomidou et al., 1989; Matesic and Lin, 1994). Animals subjected to PA showed focal swelling and marked fragmentation of MAP-2, as well as an increase in the percentage of MAP-2 reactive area. In addition, no branch or length alterations in PC dendrites were observed, as the ratio between the external and internal reactive areas resembled control values. These dendritic alterations might in part explain the increase observed in molecular layer thickness.

On the other hand, we observed an increment in internal granular layer thickness but a decrease in the number of granular cells per area in PA rats. Nevertheless, no reduction in the total number of granular layer cells in PA rats was found. This layer presented an increase in the percentage of cells with dysmorphically shaped (oval, polygonal) nuclei with speckled chromatin, as visualized by toluidine blue staining. These results are in line with those obtained in the same murine model of PA by Kohlhauser et al. who, despite finding no neuronal loss in the cerebellum, reported a remarkably elevated number of nuclei with chromatin changes (Kohlhauser et al., 1999). Taken together, our findings seem to indicate incomplete migration of granular cells generated by hypoxia and, consequently, a less compact internal granular layer.

Also, a close interaction should be noted between external granular neurons and PCs. In normal cortical development, signaling from the external granular layer is crucial to put an end to PC migration and induce the monolayer arrangement. As the settling of PCs in the cerebellar cortex is regulated by molecular signals issued

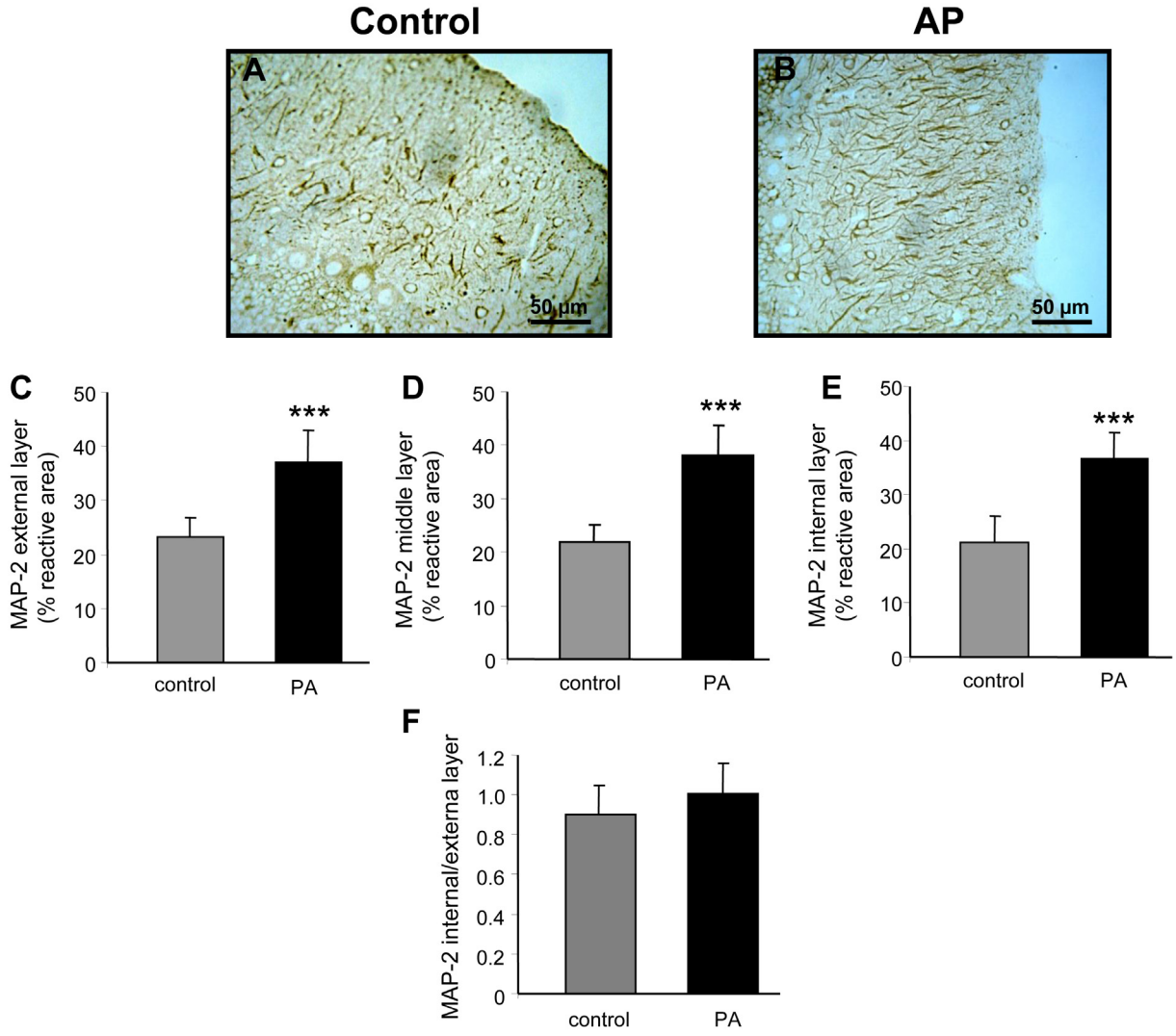

Fig. 5. Purkinje cell dendrites Panels A and B show representative microphotographs of MAP-2-stained PCs from control and PA animals, respectively. The MAP-2-positive reactive area was measured in three sub-areas of the molecular layer: external (panel C), middle (panel D) and internal (panel E). The ratio between the external and internal reactive area is shown in panel F. Data are expressed as the mean ± SD of a single experiment (Control: $n = 12$, PA: $n = 12$). ***$p < 0.001$, compared to control.

by granular cells (Carletti et al., 2008), the alterations observed in these cells could also explain PC layer disorganization.

In terms of astrocytic alterations, Western blot analyses in PA animals revealed an increase in GFAP expression, an additional well established feature of neurodegenerative damage in the CNS (Eng and Ghirnikar, 1994; Pekny and Nilsson, 2005) and a larger reactive area in both Bergmann cells and granular layer, which indicates the presence of astrogliosis and a chronic neurodegeneration process. Reactive gliosis was previously observed in other SNC area such as hypoccampus of identical age rats (P120), using the same PA model (Saraceno et al., 2010).

Cell–cell communication plays a role in specifying cell fate and regulating proper development in the formation of the cerebellar cortex. The wiring of neuronal circuits relies on precise spatial positioning of neurons and axons (Ruiz de Almodovar et al., 2010), and environmentally disturbed cell–cell interactions may result in migration problems and lead to neuron misplacement. Although cell–cell interactions are outside the scope of our work, our findings hint at PA interference with cell–cell communication and a consequent disruption in neuronal location.

Behavioural test were already made using this perinatal asphyxia model by several researcher groups (Hoeger et al., 2006; Loidl et al., 2000; Morales et al., 2010; Strackx et al., 2010; Van de Berg et al., 2003), etc.) including our group (Galeano et al., 2011). Galeanoís work, in particular, investigated the motor, emotional and cognitive functions of adult (three month old) asphyctic rats. Animals were examined in a behavioral test battery including elevated plus maze, open field, Morris water maze, and an incentive downshift procedure. The authors observed a deficit in exploration of new environments and spatial reference and working memory impairments in PA rats. Finally, when animals were downshifted from a 32% to a 4% sucrose solution, an attenuated suppression of consummatory behavior was observed in PA rats (Galeano et al., 2011). Despite of these behavioural impairment, neurological motor conditions were comparable to those of normoxic animals, in agreement with results obtained by Hoeger et al. (2006).

From a motor point of view, it should be noted that deficits, possibly linked to cerebellar lesions, are observed at very early stages ranging from days to several weeks (Young et al., 1986) but seem to be compensated 3 months after PA (Hoeger et al., 2006). These findings are in line with observations made in humans by Allin et al. who reported no correlation between the volume of the underdeveloped cerebellum in preterm children and motor function later in

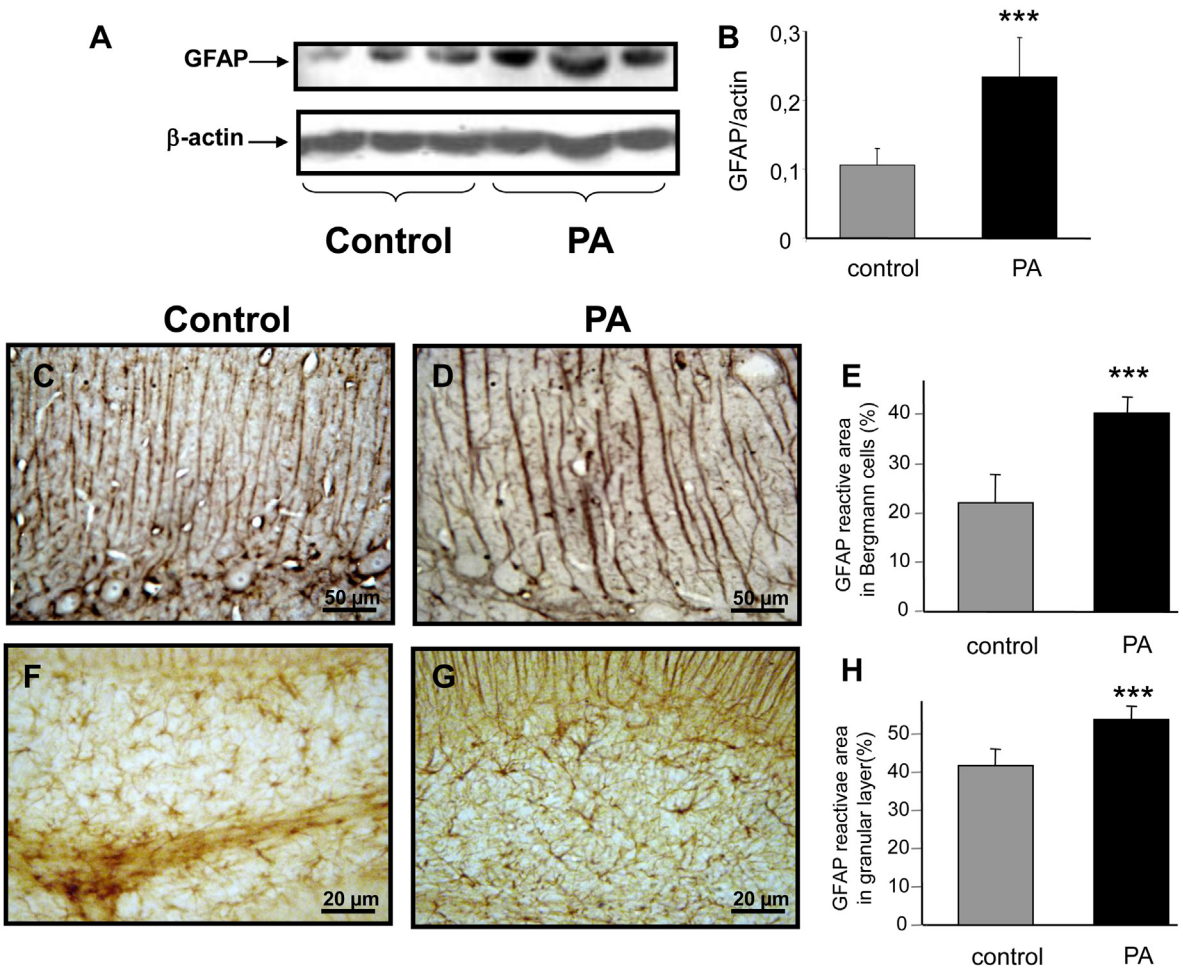

Fig. 6. Cerebellar GFAP expression. Panel A shows representative Western blot for cerebellar GFAP. Panel B shows the quantification of band intensity of three independent experiments (Control: $n = 6$, PA: $n = 6$) Panels C and D show representative microphotographs of GFAP-stained Bergman cells from control and PA animals, respectively. The measurement of the GFAP-positive reactive area is shown in panel E. Panels F and G show representative microphotographs of GFAP-stained astrocytes in the granular layer from control and PA animals, respectively. The measurement of the GFAP-positive reactive area is shown in panel H. Data are expressed as the mean ± SD of a single experiment (Control: $n = 12$, PA: $n = 12$) $^{***}p < 0.001$, compared to control.

childhood, even if cognitive and social functions remained altered (Allin et al., 2001).

Cerebellar participation in cognition and behavior is now increasingly accepted. This should not be surprising from an anatomical standpoint, as, apart from cerebellar projections to the sensorimotor cortex, homologous connections project to cognitive and affective regions and comprise a large fraction of cerebellar connectivity (Strick et al., 2009). In addition to its role in the mature brain, the cerebellum acts in early life to shape the function of other brain regions, especially those relating to cognition and affection. Neonatal damage to the cerebellum can have persistent structural and functional consequences. In particular, damage due to premature birth or as a consequence of surgery produces social deficits (Bolduc et al., 2012). For example, it has been established that an early disruption of the cerebellar circuitry is positively correlated with autism (Limperopoulos et al., 2007).

In conclusion, this work shows long-term effects of PA on cerebellar structure, which could be involved in the pathogenesis of cognitive deficits observed in both animals and humans.

Conflict of interest

The authors declare no conflicts of interest.

Acknowledgements

This work was supported by the National Scientific and Technical Research Council (PIP 11420100100159, CONICET, Argentina) to FC, and the University of Buenos Aires (UBACYT 20020090100118) to FC. SR and TL are fellowship holders from the National Scientific and Technical Research Council (CONICET, Argentina).

References

Allin, M., Matsumoto, H., Santhouse, A.M., Nosarti, C., AlAsady, M.H., Stewart, A.L., Rifkin, L., Murray, R.M., 2001. Cognitive and motor function and the size of the cerebellum in adolescents born very pre-term. Brain 124, 60–66.

Anderson, V., Spencer-Smith, M., Wood, A., 2011. Do children really recover better? Neurobehavioural plasticity after early brain insult. Brain 134, 2197–2221.

Barks, J.D., Silverstein, F.S., 1992. Excitatory amino acids contribute to the pathogenesis of perinatal hypoxic-ischemic brain injury. Brain Pathol. 2, 235–243.

Biran, V., Heine, V.M., Verney, C., Sheldon, R.A., Spadafora, R., Vexler, Z.S., Rowitch, D.H., Ferriero, D.M., 2011. Cerebellar abnormalities following hypoxia alone compared to hypoxic-ischemic forebrain injury in the developing rat brain. Neurobiol. Dis. 41, 138–146.

Biran, V., Verney, C., Ferriero, D.M., 2012. Perinatal cerebellar injury in human and animal models. Neurol. Res. Int. 2012, 858929.

Bjelke, B., Andersson, K., Ogren, S.O., Bolme, P., 1991. Asphyctic lesion: proliferation of tyrosine hydroxylase-immunoreactive nerve cell bodies in the rat substantia nigra and functional changes in dopamine neurotransmission. Brain Res. 543, 1–9.

Bolduc, M.E., du Plessis, A.J., Sullivan, N., Guizard, N., Zhang, X., Robertson, R.L., Limperopoulos, C., 2012. Regional cerebellar volumes predict functional outcome in children with cerebellar malformations. Cerebellum 11, 531–542.
Capani, F., Loidl, C.F., Aguirre, F., Piehl, L., Facorro, G., Hager, A., De Paoli, T., Farach, H., Pecci-Saavedra, J., 2001. Changes in reactive oxygen species (ROS) production in rat brain during global perinatal asphyxia: an ESR study. Brain Res. 914, 204–207.
Capani, F., Saraceno, G.E., Botti, V., Aon-Bertolino, L., de Oliveira, D.M., Barreto, G., Galeano, P., Giraldez-Alvarez, L.D., Coirini, H., 2009. Protein ubiquitination in postsynaptic densities after hypoxia in rat neostriatum is blocked by hypothermia. Exp. Neurol. 219, 404–413.
Carletti, B., Williams, I.M., Leto, K., Nakajima, K., Magrassi, L., Rossi, F., 2008. Time constraints and positional cues in the developing cerebellum regulate Purkinje cell placement in the cortical architecture. Dev. Biol. 317, 147–160.
Celio, M.R., 1990. Calbindin D-28k and parvalbumin in the rat nervous system. Neuroscience 35, 375–475.
Cervos-Navarro, J., Sampaolo, S., Hamdorf, G., 1991. Brain changes in experimental chronic hypoxia. Exp. Pathol. 42, 205–212.
Cheng, Y., Deshmukh, M., D'Costa, A., Demaro, J.A., Gidday, J.M., Shah, A., Sun, Y., Jacquin, M.F., Johnson, E.M., Holtzman, D.M., 1998. Caspase inhibitor affords neuroprotection with delayed administration in a rat model of neonatal hypoxic-ischemic brain injury. J. Clin. Invest. 101, 1992–1999.
de Haan, M., Wyatt, J.S., Roth, S., Vargha-Khadem, F., Gadian, D., Mishkin, M., 2006. Brain and cognitive-behavioural development after asphyxia at term birth. Dev. Sci. 9, 350–358.
Dorfman, V.B., Vega, M.C., Coirini, H., 2006. Age-related changes of the GABA-B receptor in the lumbar spinal cord of male rats and penile erection. Life Sci. 78, 1529–1534.
du Plessis, A.J., Volpe, J.J., 2002. Perinatal brain injury in the preterm and term newborn. Curr. Opin. Neurol. 15, 151–157.
Eng, L.F., Ghirnikar, R.S., 1994. GFAP and astrogliosis. Brain Pathol. 4, 229–237.
Galeano, P., Blanco Calvo, E., Madureira de Oliveira, D., Cuenya, L., Kamenetzky, G.V., Mustaca, A.E., Barreto, G.E., Giraldez-Alvarez, L.D., Milei, J., Capani, F., 2011. Long-lasting effects of perinatal asphyxia on exploration, memory and incentive downshift. Int. J. Dev. Neurosci. 29, 609–619.
Ghez, C., Fahn, S., 1985. The cerebellum. In: Principles of Neural Science. Elsevier, New York, pp. 502–522.
Glickstein, M., 2006. Thinking about the cerebellum. Brain 129, 288–290.
Gonzalez, F.F., Ferriero, D.M., 2008. Therapeutics for neonatal brain injury. Pharmacol. Ther. 120, 43–53.
Hagan, P., Barks, J.D., Yabut, M., Davidson, B.L., Roessler, B., Silverstein, F.S., 1996. Adenovirus-mediated over-expression of interleukin-1 receptor antagonist reduces susceptibility to excitotoxic brain injury in perinatal rats. Neuroscience 75, 1033–1045.
Hoeger, H., Engidawork, E., Stolzlechner, D., Bubna-Littitz, H., Lubec, B., 2006. Long-term effect of moderate and profound hypothermia on morphology, neurological, cognitive and behavioural functions in a rat model of perinatal asphyxia. Amino Acids 31, 385–396.
Hori, N., Carpenter, D.O., 1994. Functional and morphological changes induced by transient in vivo ischemia. Exp. Neurol. 129, 279–289.
Hsu, M., Buzsaki, G., 1993. Vulnerability of mossy fiber targets in the rat hippocampus to forebrain ischemia. J. Neurosci. 13, 3964–3979.
Ikonomidou, C., Price, M.T., Mosinger, J.L., Frierdich, G., Labruyere, J., Salles, K.S., Olney, J.W., 1989. Hypobaric-ischemic conditions produce glutamate-like cytopathology in infant rat brain. J. Neurosci. 9, 1693–1700.
Katsetos, C.D., Spandou, E., Legido, A., Taylor, M.L., Zanelli, S.A., de Chadarevian, J.P., Christakos, S., Mishra, O.P., Delivoria-Papadopoulos, M., 2001. Acute hypoxia-induced alterations of calbindin-D28k immunoreactivity in cerebellar Purkinje cells of the guinea pig fetus at term. J. Neuropathol. Exp. Neurol. 60, 470–482.
Kaufman, S.A., Miller, S.P., Ferriero, D.M., Glidden, D.H., Barkovich, A.J., Partridge, J.C., 2003. Encephalopathy as a predictor of magnetic resonance imaging abnormalities in asphyxiated newborns. Pediatr. Neurol. 28, 342–346.
Kinney, D.K., Munir, K.M., Crowley, D.J., Miller, A.M., 2008. Prenatal stress and risk for autism. Neurosci. Biobehav. Rev. 32, 1519–1532.
Kohlhauser, C., Kaehler, S., Mosgoeller, W., Singewald, N., Kouvelas, D., Prast, H., Hoeger, H., Lubec, B., 1999. Histological changes and neurotransmitter levels three months following perinatal asphyxia in the rat. Life Sci. 64, 2109–2124.
Laure-Kamionowska, M., Maslinska, D., 2011. Cerebellar cortical neurons misplaced in the white matter due to disturbed migration during development of human brain. Folia Neuropathol. 49, 282–294.
Lawn, J.E., Cousens, S., Zupan, J., 2005. 4 million neonatal deaths: when? Where? Why? Lancet 365, 891–900.
Limperopoulos, C., Soul, J.S., Gauvreau, K., Huppi, P.S., Warfield, S.K., Bassan, H., Robertson, R.L., Volpe, J.J., du Plessis, A.J., 2005. Late gestation cerebellar growth is rapid and impeded by premature birth. Pediatrics 115, 688–695.
Limperopoulos, C., Bassan, H., Gauvreau, K., Robertson Jr., R.L., Sullivan, N.R., Benson, C.B., Avery, L., Stewart, J., Soul, J.S., Ringer, S.A., Volpe, J.J., duPlessis, A.J., 2007. Does cerebellar injury in premature infants contribute to the high prevalence of long-term cognitive, learning, and behavioral disability in survivors? Pediatrics 120, 584–593.
Liu, X.H., Eun, B.L., Silverstein, F.S., Barks, J.D., 1996. The platelet-activating factor antagonist BN 52,021 attenuates hypoxic-ischemic brain injury in the immature rat. Pediatr. Res. 40, 797–803.
Loidl, C.F., Gavilanes, A.W., Van Dijk, E.H., Vreuls, W., Blokland, A., Vles, J.S., Steinbusch, H.W., Blanco, C.E., 2000. Effects of hypothermia and gender on survival and behavior after perinatal asphyxia in rats. Physiol. Behav. 68, 263–269.
Matesic, D.F., Lin, R.C., 1994. Microtubule-associated protein 2 as an early indicator of ischemia-induced neurodegeneration in the gerbil forebrain. J. Neurochem. 63, 1012–1020.
McEwen, B.S., 2007. Physiology and neurobiology of stress and adaptation: central role of the brain. Physiol. Rev. 87, 873–904.
Miale, I.L., Sidman, R.L., 1961. An autoradiographic analysis of histogenesis in the mouse cerebellum. Exp. Neurol. 4, 277–296.
Miller, S.P., Ferriero, D.M., 2009. From selective vulnerability to connectivity: insights from newborn brain imaging. Trends Neurosci. 32, 496–505.
Morales, P., Simola, N., Bustamante, D., Lisboa, F., Fiedler, J., Gebicke-Haerter, P.J., Morelli, M., Tasker, R.A., Herrera-Marschitz, M., 2010. Nicotinamide prevents the long-term effects of perinatal asphyxia on apoptosis, non-spatial working memory and anxiety in rats. Exp. Brain Res. 202, 1–14.
O'Lone, R., Knorr, K., Jaffe, I.Z., Schaffer, M.E., Martini, P.G., Karas, R.H., Bienkowska, J., Mendelsohn, M.E., Hansen, U., 2007. Estrogen receptors alpha and beta mediate distinct pathways of vascular gene expression, including genes involved in mitochondrial electron transport and generation of reactive oxygen species. Mol. Endocrinol. 21, 1281–1296.
Odd, D.E., Lewis, G., Whitelaw, A., Gunnell, D., 2009. Resuscitation at birth and cognition at 8 years of age: a cohort study. Lancet 373, 1615–1622.
Pekny, M., Nilsson, M., 2005. Astrocyte activation and reactive gliosis. Glia 50, 427–434.
Rakic, P., Sidman, R.L., 1970. Histogenesis of cortical layers in human cerebellum, particularly the lamina dissecans. J. Comp. Neurol. 139, 473–500.
Rice, D., Barone Jr., S., 2000. Critical periods of vulnerability for the developing nervous system: evidence from humans and animal models. Environ. Health Perspect. 108 (Suppl. 3), 511–533.
Ruiz de Almodovar, C., Coulon, C., Salin, P.A., Knevels, E., Chounlamountri, N., Poesen, K., Hermans, K., Lambrechts, D., Van Geyte, K., Dhondt, J., Dresselaers, T., Renaud, J., Aragones, J., Zacchigna, S., Geudens, I., Gall, D., Stroobants, S., Mutin, M., Dassonville, K., Storkebaum, E., Jordan, B.F., Eriksson, U., Moons, L., D'Hooge, R., Haigh, J.J., Belin, M.F., Schiffmann, S., Van Hecke, P., Gallez, B., Vinckier, S., Chedotal, A., Honnorat, J., Thomasset, N., Carmeliet, P., Meissirel, C., 2010. Matrix-binding vascular endothelial growth factor (VEGF) isoforms guide granule cell migration in the cerebellum via VEGF receptor Flk1. J. Neurosci. 30, 15052–15066.
Saraceno, G.E., Bertolino, M.L., Galeano, P., Romero, J.I., Garcia-Segura, L.M., Capani, F., 2010. Estradiol therapy in adulthood reverses glial and neuronal alterations caused by perinatal asphyxia. Exp. Neurol. 223, 615–622.
Seidl, R., Stockler-Ipsiroglu, S., Rolinski, B., Kohlhauser, C., Herkner, K.R., Lubec, B., Lubec, G., 2000. Energy metabolism in graded perinatal asphyxia of the rat. Life Sci. 67, 421–435.
Strackx, E., Van den Hove, D.L., Prickaerts, J., Zimmermann, L., Steinbusch, H.W., Blanco, C.E., Gavilanes, A.W., Vles, J.S., 2010. Fetal asphyctic preconditioning protects against perinatal asphyxia-induced behavioral consequences in adulthood. Behav. Brain Res. 208, 343–351.
Strick, P.L., Dum, R.P., Fiez, J.A., 2009. Cerebellum and nonmotor function. Annu. Rev. Neurosci. 32, 413–434.
ten Donkelaar, H.J., Lammens, M., Wesseling, P., Thijssen, H.O., Renier, W.O., 2003. Development and developmental disorders of the human cerebellum. J. Neurol. 250, 1025–1036.
Titomanlio, L., Kavelaars, A., Dalous, J., Mani, S., El Ghouzzi, V., Heijnen, C., Baud, O., Gressens, P., 2011. Stem cell therapy for neonatal brain injury: perspectives and challenges. Ann. Neurol. 70, 698–712.
Van de Berg, W.D., Kwaijtaal, M., de Louw, A.J., Lissone, N.P., Schmitz, C., Faull, R.L., Blokland, A., Blanco, C.E., Steinbusch, H.W., 2003. Impact of perinatal asphyxia on the GABAergic and locomotor system. Neuroscience 117, 83–96.
Van Erp, T.G., Saleh, P.A., Rosso, I.M., Huttunen, M., Lonnqvist, J., Pirkola, T., Salonen, O., Valanne, L., Poutanen, V.P., Standertskjold-Nordenstam, C.G., Cannon, T.D., 2002. Contributions of genetic risk and fetal hypoxia to hippocampal volume in patients with schizophrenia or schizoaffective disorder, their unaffected siblings, and healthy unrelated volunteers. Am. J. Psychiatry 159, 1514–1520.
Vannucci, S.J., Hagberg, H., 2004. Hypoxia-ischemia in the immature brain. J. Exp. Biol. 207, 3149–3154.
Verger, K., Junque, C., Levin, H.S., Jurado, M.A., Perez-Gomez, M., Bartres-Faz, D., Barrios, M., Alvarez, A., Bartumeus, F., Mercader, J.M., 2001a. Correlation of atrophy measures on MRI with neuropsychological sequelae in children and adolescents with traumatic brain injury. Brain Inj. 15, 211–221.
Verger, K., Serra-Grabulosa, J.M., Junque, C., Alvarez, A., Bartres-Faz, D., Mercader, J.M., 2001b. Study of the long term sequelae of traumatic brain injury: evaluation of declarative and procedural memory, and its neuroanatomic substrate. Rev. Neurol. 33, 30–34.
Volpe, J.J., 2009. Cerebellum of the premature infant: rapidly developing, vulnerable, clinically important. J. Child Neurol. 24, 1085–1104.
Wang, V.Y., Zoghbi, H.Y., 2001. Genetic regulation of cerebellar development. Nat. Rev. Neurosci. 2, 484–491.

Welsh, J.P., Yuen, G., Placantonakis, D.G., Vu, T.Q., Haiss, F., O'Hearn, E., Molliver, M.E., Aicher, S.A., 2002. Why do Purkinje cells die so easily after global brain ischemia? Aldolase C, EAAT4, and the cerebellar contribution to posthypoxic myoclonus. Adv. Neurol. 89, 331–359.
Yager, J.Y., Thornhill, J.A., 1997. The effect of age on susceptibility to hypoxic-ischemic brain damage. Neurosci. Biobehav. Rev. 21, 167–174.
Young, R.S., Kolonich, J., Woods, C.L., Yagel, S.K., 1986. Behavioral performance of rats following neonatal hypoxia-ischemia. Stroke 17, 1313–1316.
Zervas, M., Blaess, S., Joyner, A.L., 2005. Classical embryological studies and modern genetic analysis of midbrain and cerebellum development. Curr. Top. Dev. Biol. 69, 101–138.